NASA TECHNICAL NOTE

NASA TN D-5732

NASA TN D-5732

EFFECTS OF NUCLEAR RADIATION ON A HIGH-RELIABILITY SILICON POWER DIODE

II - Analysis of Forward Electrical Characteristics

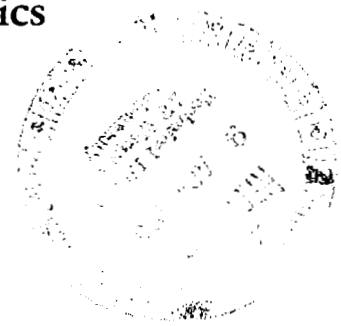

by Julian F. Been

Lewis Research Center
Cleveland, Ohio

NATIONAL AERONAUTICS AND SPACE ADMINISTRATION • WASHINGTON, D. C. • APRIL 1970

1. Report No. NASA TN D-5732	2. Government Accession No.	3. Recipient's Catalog No.
4. Title and Subtitle EFFECTS OF NUCLEAR RADIATION ON A HIGH-RELIABILITY SILICON POWER DIODE II - ANALYSIS OF FORWARD ELECTRICAL CHARACTERISTICS		5. Report Date April 1970 6. Performing Organization Code
7. Author(s) Julian F. Been		8. Performing Organization Report No. E-5296
9. Performing Organization Name and Address Lewis Research Center National Aeronautics and Space Administration Cleveland, Ohio 44135		10. Work Unit No. 120-27 11. Contract or Grant No. 13. Type of Report and Period Covered
12. Sponsoring Agency Name and Address National Aeronautics and Space Administration Washington, D. C. 20546		Technical Note 14. Sponsoring Agency Code

15. Supplementary Notes

16. Abstract

One hundred power diodes were irradiated in the NASA Plum Brook Reactor. The changes in forward electrical characteristics due to nuclear radiation were interpreted in terms of decreasing minority carrier lifetimes. The increase in forward voltage at high current densities was the most significant change. The pre- and post-irradiation data were analyzed in terms of n^+-p-p^+-type junction theory. The critical quantity was the ratio of the base width to the high-level diffusion length. Control of the ratio suggests a means of increasing the radiation tolerance of this type diode. The effects of space-charge limiting were also considered.

17. Key Words (Suggested by Author(s))

Silicon
Power
Diodes
Nuclear irradiation
Forward biased

18. Distribution Statement

Unclassified - unlimited

19. Security Classif. (of this report)	20. Security Classif. (of this page)	21. No. of Pages	22. Price *
Unclassified	Unclassified	27	$3.00

*For sale by the Clearinghouse for Federal Scientific and Technical Information Springfield, Virginia 22151

EFFECTS OF NUCLEAR RADIATION ON A HIGH-RELIABILITY SILICON POWER DIODE
II - ANALYSIS OF FORWARD ELECTRICAL CHARACTERISTICS

by Julian F. Been
Lewis Research Center

SUMMARY

An analysis of the effects of nuclear radiation on the forward electrical characteristics of a 35-ampere, 500-peak-inverse-voltage, high-reliability silicon power diode is presented. The forward electrical characteristics before and after irradiation of the diodes in the NASA Plum Brook Reactor are discussed in terms of changes in minority carrier lifetimes. The most significant operating region of the forward characteristics was at currents in the ampere range. In this region, each diode showed a considerable increase in the forward voltage drop for a given current. However, the magnitude of the increase varied considerably among the diodes. These results agree with a theory of Shields which predicts that, for this type junction (n^+-p-p^+), the critical parameter in determining the forward voltage drop is the geometric ratio of the base width to the high-level diffusion length. Control of this ratio during fabrication thus offers a method of increasing the radiation tolerance of the diodes as to the magnitude of change as well as minimizing differences among the characteristics of the diodes. Another important control is the p-base doping level, which would reduce space-charge limiting after irradiation. The low-level current-voltage characteristics agreed reasonably well with existing p-n junction theory.

INTRODUCTION

In nuclear electric power generating systems proposed for space applications, the electrical components most sensitive to nuclear radiation are the semiconductor devices. Changes in their electrical characteristics can limit the lifetime of the entire power

generating system. It is therefore necessary to establish which of these electrical characteristics change enough to affect the reliability of the system and, where possible, to correlate these changes with the basic properties of the device. This type of correlation requires detailed experimental and analytical study. Through this correlation and analysis, an understanding is established whereby more radiation-resistant semiconductors can be designed, including multijunction devices such as transistors and silicon-controlled rectifiers. These improved devices would allow optimum system design with minimum shielding and yet be consistent with reliability requirements.

The effects most usually observed when semiconductors are subjected to nuclear radiation are increases in reverse leakage currents, increases in forward voltage drop for a given current, decreases in current gain in transistors, and increases in gate current and voltage requirements in controlled rectifiers. These changes with radiation cause lowered power-conditioning efficiency and an increased waste heat. Although alternative devices to semiconductors exist, such as gas-filled or vacuum tubes, these are, in general, heavier, require more power, and are less reliable.

The literature on radiation effects on semiconductor devices is extensive. The emphasis, however, has been on small, low-power, low-voltage devices, with very little work reported on the high-current, high-peak-inverse-voltage region of interest for power conditioning in space electric power systems. Messenger et al. (ref. 1) has summarized much of this work on low-power devices. Larin's work (ref. 2) deals also almost entirely with low-power devices. The present report is concerned with understanding the change in the forward current-voltage characteristics of a 35-ampere, 500-peak-inverse-voltage, silicon power diode with exposure to nuclear radiation. This study is part of a larger program under way at the Lewis Research Center to investigate the effects of nuclear radiation on silicon devices applicable to nuclear electric space power sources. A report (ref. 3) was prepared for the use of circuit designers and others interested in the effects of radiation on the current-voltage characteristics (an analysis of the data was omitted). The present report provides a comparison of the experimental data with theoretical predictions for the forward-bias region.

DESCRIPTION OF DIODES TESTED

The diode investigated was an S1N1189. The prefix "S" in the part number indicates that the diode passed the NASA Marshall Space Flight Center screening and performance specification (ref. 4). The silicon chip configuration is shown in figure 1 and has an n^+-p-p^+-type junction prepared by a double-diffusion process. The base region p-material is doped to 1.4×10^{14} to 2.0×10^{14} boron atoms per cubic centimeter. The p^+-region has a surface dopant concentration of 1.0×10^{19} boron atoms per cubic centi-

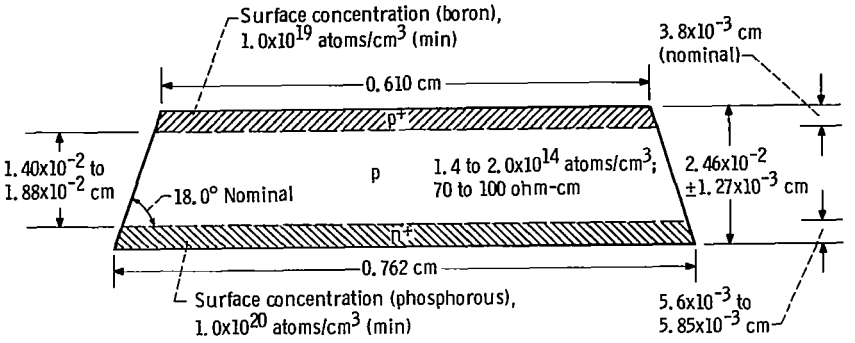

Figure 1. - Silicon chip configuration of S1N1189. Drawing not to scale.

timeter (min). The nominal depth of the p-p^+ junction is 38 micrometers. The n^+-region has a surface dopant concentration of 1.0×10^{20} phosphorous atoms per cubic centimeter (min) with a nominal n^+-p junction depth of 57 micrometers. The chip is circular with sides beveled to a nominal 18^o slope, which lowers the electric field at the surface (ref. 5). The beveled sides are coated with a silicone rubber to form a passivation layer on the surface. The nominal diameter of the chip on the p^+-side is 0.61 centimeter and is 0.76 centimeter on the n^+-side. The overall thickness of the chip is approximately 2.54×10^{-2} centimeter.

DESCRIPTION OF IRRADIATION

The two factors expected to be most important in modifying the damage due to nuclear radiation in an operating space power system are the operating temperature and current.

The irradiation testing of the diodes actually consisted of two separate tests. In each, 50 diodes were irradiated simultaneously in the reactor under similar conditions, with the important difference being the temperature at which the two sets of diodes were irradiated. Each test set of 50 diodes was divided into groups according to the operating modes given in table I. Operating currents and voltages were determined primarily by normal derating at the lower temperatures.

All diodes in each test were operated in the modes (table I) during irradiation except when measurements were taken. The irradiation of each test set proceeded for two reactor cycles, the nominal reactor cycle being 10 days at rated power, depending on the reactor power scheduling. The average temperatures of the diodes during irradiation (table I) were different for the three operating groups because one coolant line served all the diodes on each test plate, and each diode was its own heat source. For example, the reverse-biased group generated less heat than the forward-biased group and therefore operated at lower temperatures. Table I also includes the change in average oper-

TABLE I. - DIODE GROUPING FOR EACH TEST BY OPERATING MODES WITH AVERAGE INITIAL AND FINAL IRRADIATION TEMPERATURES

Group	Diodes per set	Operating mode	Set			
			I		II	
			Neutron fluence, neutrons/cm^2			
			4.6×10^{13}		4.0×10^{13}	
			Average temperature, T, ^{o}C			
			Initial	Final	Initial	Final
A	10	Forward current, 10 A dc	48.5	60	106	125
B	10	Reverse biased, 100 V dc	38	43	103	102
C	30	ac rectification; average forward current, 10 A; peak reverse voltage, 150 V	50.5	66	99	124
Total	50	----------	----	60	---	120

ating temperatures as each test progressed. As used in this report, designated nominal temperatures represent the average final temperature.

The first set of diodes (test I, 60^{o} C nominal) received a fast-neutron ($\geq$0.1 MeV) fluence of $4.6\pm1.5\times10^{13}$ neutrons per square centimeter, and the second set of diodes (test II, 120^{o} C nominal) received $4.9\pm1.6\times10^{13}$ neutrons per square centimeter (ref. 6). The gamma dosage for each set of diodes was $3.2\pm0.6\times10^{7}$ rads (C).

The methods for determining the fast-neutron flux and gamma dosage and the conditions for which a calculated flux can be obtained are described in references 6 and 7.

COMPARISON OF MEASURED AND CALCULATED DIODE CURRENT-VOLTAGE CHARACTERISTICS FOR UNIRRADIATED DIODES

The 100 diodes to be irradiated were divided into two tests of 50 each. Current-voltage characteristics of the first set of diodes are given before irradiation in figure 2.

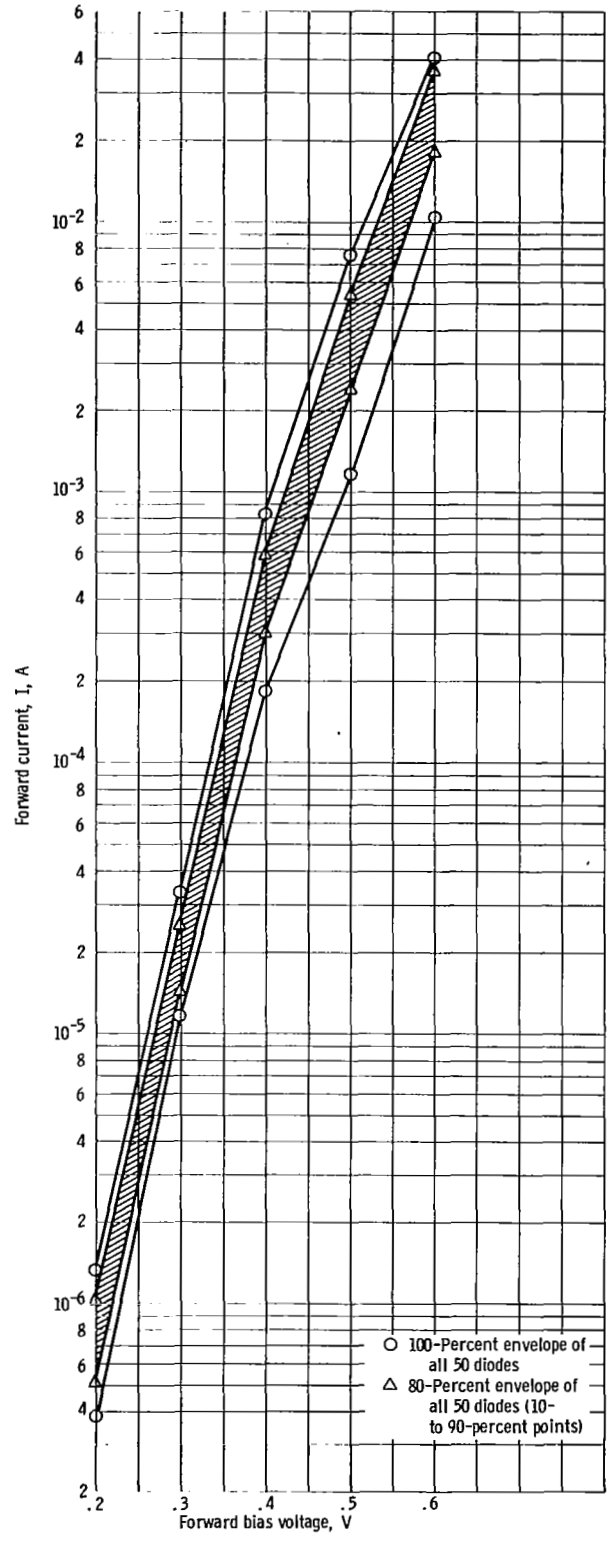

Figure 2. - Test I, before irradiation. Envelope of currents for all test diodes as function of forward bias voltage.

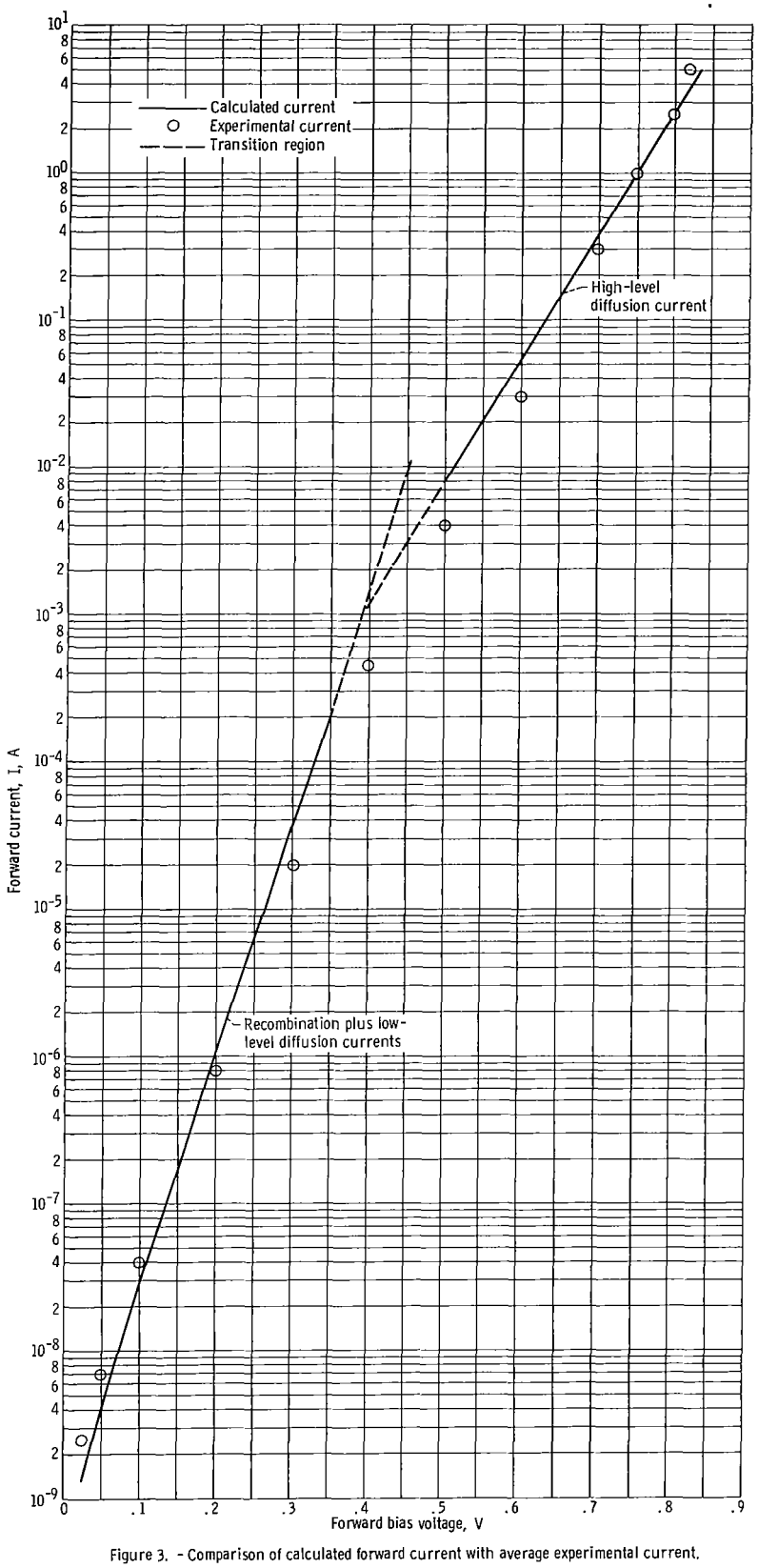

Figure 3. - Comparison of calculated forward current with average experimental current.

Five decades of current from 7×10^{-7} to 2×10^{-2} ampere are covered. This figure demonstrates the variation found in a set of diodes with the same part number and manufactured by the same process. The 80- and 100-percent envelopes of the diode characteristics are plotted. The upper and lower 100-percent envelopes of current represent approximately the $2I_{ave}$ and $\frac{1}{2}I_{ave}$, respectively. The second set of 50 diodes has about the same variation as that in the first 50. For currents larger than shown in figure 2 (applied voltages > 0.6 V), the variations continue to be about the same (i.e., the 100-percent upper and lower envelopes are about a factor of 2 removed from the average). For voltages lower than those in figure 2 (i.e., in the mV range), the variations become larger, probably because of surface effects. A current-voltage curve for the arithmetical average of the 50 diodes is given in figure 3. Data are not shown above 5 amperes because of the difficulty of correcting for junction heating.

With the use of recombination-generation and diffusion theories, the current was calculated over a range of 8 orders of magnitude. Details of this analysis are in appendix B. (Symbols are defined in appendix A.) Figure 3 gives the calculated and measured currents as a function of applied voltages of 25 millivolts and above. The calculations and the experimental average agree to within a factor of 2 over this current range. Thus, within these limits, the calculated currents may be said to be in fair agreement with measured values.

The fact that agreement is obtained over 8 decades indicates that some confidence can be placed in the theoretical approach and parameters used. The preirradiation values for the basic diode parameters used in the calculations were

(1) Carrier lifetime at low injection levels, 5×10^{-6} second (obtained from the manufacturer)

(2) Built-in voltage, 0.35 volt (obtained by author from capacitance-voltage measurements)

(3) Voltage drop in the base at high current levels, 0.116 volt (estimated from experimental data, appendix B)

(4) High-level diffusion length, 6.5×10^{-3} centimeter (obtained from calculations)

This agreement between theory and experiment provides a basis for comparison of currents before and after irradiation. Closer agreement between theory and measured values would require very careful control of diode construction and a better knowledge of such parameters as minority carrier lifetime as well as a more accurate theory.

EFFECTS OF IRRADIATION ON ELECTRICAL CHARACTERISTICS

Effect of Operating Mode and Operating Temperature on Radiation Damage

As stated in the previous section, each test set was divided into three groups during irradiation according to the following operating modes:

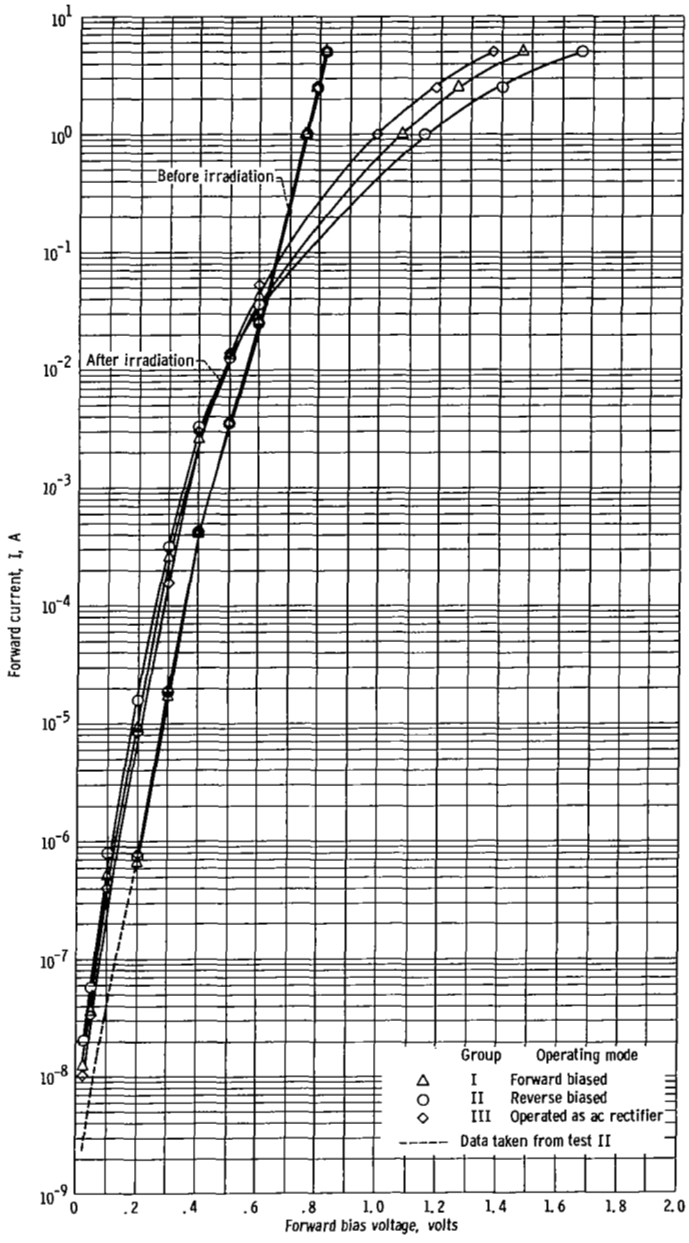

Figure 4. - Average values of forward current as function of voltage according to operating modes for test I (60° C nominal). Neutron fluence, 4.6×10^{13} neutrons per square centimeter.

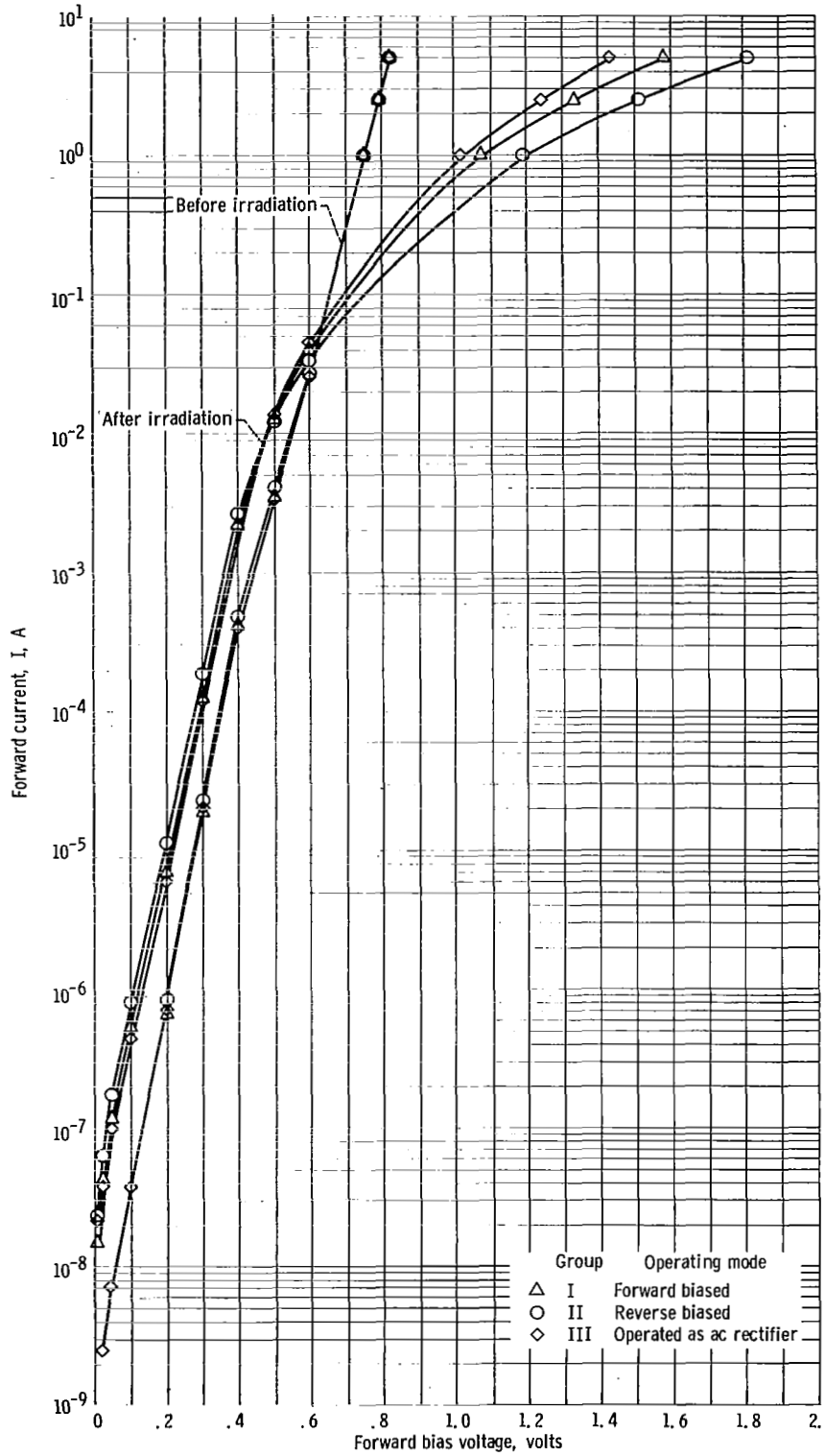

Figure 5. - Average values of forward current voltage according to operating modes for test II (120° C nominal). Neutron fluence, 4.9×10^{13} neutrons per square centimeter.

(1) Forward current, 10 amperes A dc, 10 diodes

(2) Reverse bias, 100 volts dc, 10 diodes

(3) Alternating-current rectification, average forward current 10 amperes, peak reverse voltage 150 volts, 30 diodes

The average values of the characteristics for each of these groups are given in figures 4 and 5. The average currents for the unirradiated diodes are also included for reference. Below a transition voltage of about 0.6 volt, the current increases with radiation, while above the transition voltage, the current decreases. Regardless of the operating mode, above 0.6 volt, all diodes showed a decrease in current although the smallest change occurred in mode C (ac rectifiers). The next larger change occurred in mode A (10 A dc), and the largest change occurred in mode B (reverse bias).

An estimate of the effect of temperature can be obtained from a ratio of the average currents for the two sets (see table II). The ratio has a maximum value at low currents, goes through a minimum, and rises again at high currents. The net effect of operating temperature is, at most, of marginal significance, and more definitive information would require much larger sample sizes as well as much more closely controlled diode manufacturing. For the purpose of this report, the effect of operating temperature during irradiation will be considered negligible.

TABLE II. - EFFECT OF OPERATING TEMPERATURE DURING DIODE IRRADIATION

Voltage, V	Average current,[a] I_{ave}, A, for diodes irradiated at -		$\frac{i\ 60^{\circ}\ C}{i\ 120^{\circ}\ C}$
	60° C	120° C	
0.1	4×10^{-7}	6.0×10^{-7}	0.7
.2	1.2×10^{-5}	8.3×10^{-6}	1.4
.3	2.2×10^{-4}	1.6×10^{-4}	1.4
.4	2.7×10^{-3}	2.3×10^{-3}	1.2
.5	1.4×10^{-2}	1.3×10^{-2}	1.1
.6	3.7×10^{-2}	4.1×10^{-2}	.9
.7	9.0×10^{-2}	9.1×10^{-2}	1.0
.8	2.1×10^{-1}	1.9×10^{-1}	1.1
1.0	7.4×10^{-1}	6.4×10^{-1}	1.2
1.2	2.0	1.6	1.3
1.4	4.1	3.1	1.3

[a]Currents were averaged over the three operating modes and were measured at room temperature.

Radiation Damage at Very Low Applied Voltages

For applied voltage in the range of a few millivolts, the current-voltage I-V relation is linear, as predicted by both generation-recombination and diffusion theories. See equation (B1) in appendix B for small voltages. This linearity, which also extends to negative voltages, is shown in figure 6 along with the results of two reactor irradiations on the diode characteristics. These curves only indicate the qualitative nature of the I-V

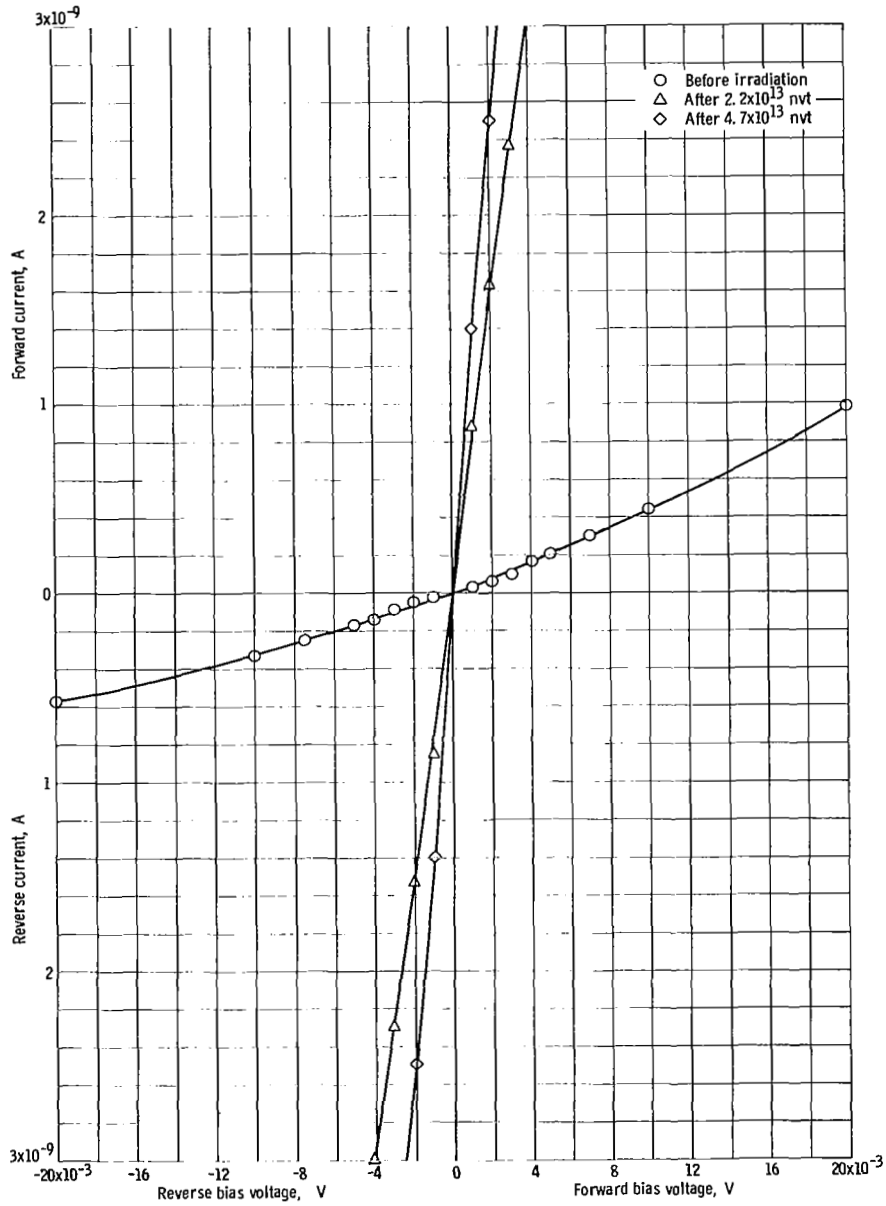

Figure 6. - Diode 879 current-voltage characteristics for small bias voltage.

TABLE III. - EFFECTS OF RADIATION ON S1N1189

DIODES FOR 2-mV APPLIED VOLTAGE

Diode	Unirradiated	Irradiated to 2.2×10^{13} N/cm^2	Irradiated to 4.7×10^{13} N/cm^2
	Diode current, I, A		
879	6×10^{-11}	1.6×10^{-9}	2.5×10^{-9}
878	8	1.3	1.8
748	18	2.6	4.4
844	70	2.2	2.8

interdependence since wide quantitative variations were found in unirradiated diode characteristics at these low voltage levels. Table III compares the results of the irradiation of four arbitrarily selected diodes and shows that all these diodes had reasonably linear current-voltage characteristics up to about 5 millivolts. Thus, it is sufficient to compare results at one voltage point. This wide variation between the unirradiated diodes tends to disappear as the leakage currents increased with increasing fast-neutron fluence. Since the wide variations were probably due to surface effects, no analysis was attempted in this voltage region.

Radiation Damage at Medium- and High-Current Ranges

Figures 4 and 5 are plots of average values of current according to operating modes against forward-bias voltage. These plots illustrate very well the effects that operating modes have on the amount of change in the diode electrical characteristics during operation in a nuclear environment. However, the considerable spread in the forward voltage drops for given currents after irradiation are best seen in figures 7 and 8, which are plots for all diodes on the basis of 0 to 100 and 10 to 90 percent of the forward current as a function of voltage. These curves illustrate the considerable spread in the forward voltage drops for given currents after irradiation. Figure 9 shows the effects of irradiation for each mode separately. Several general statements can be made from examining figures 4 to 9:

(1) The bias region in which the current showed the largest change with radiation was the very low millivolt range (see fig. 6).

(2) The curves are no longer straight lines above approximately 0.5 volt on a log-linear plot, which indicates that after irradiation the current is no longer a truly exponential function of the applied voltage (see figs. 5 and 6).

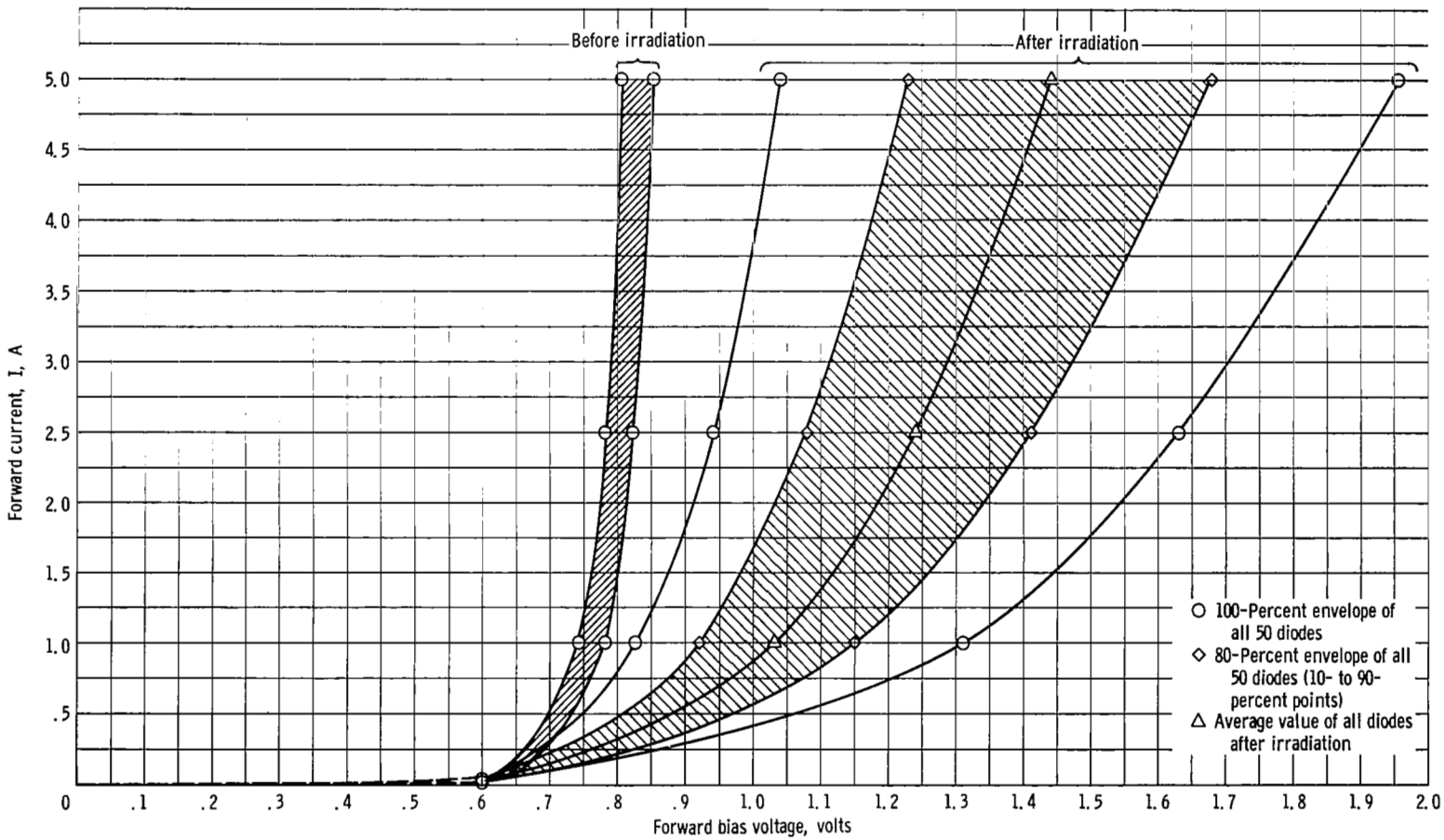

Figure 7. - Forward currents as function of voltage of all diodes before and after irradiation for test I. Temperature, 60° C nominal; neutron fluence, 4.6×10^{13} neutrons per square centimeter.

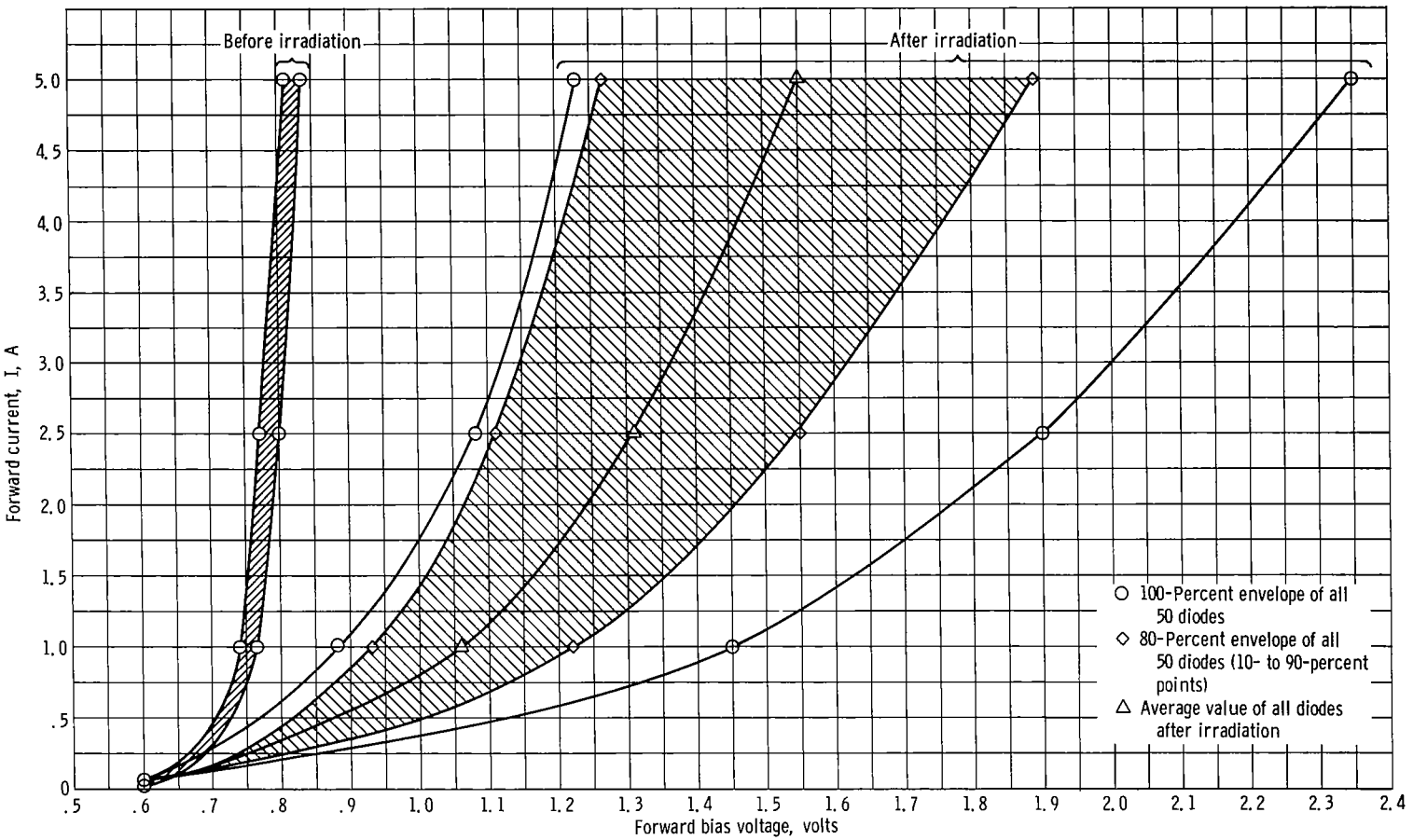

Figure 8. - Forward currents as function of voltage of all diodes before and after irradiation for test II. Temperature, 125° C nominal; neutron fluence, 4.9×10^{13} neutrons per square centimeter.

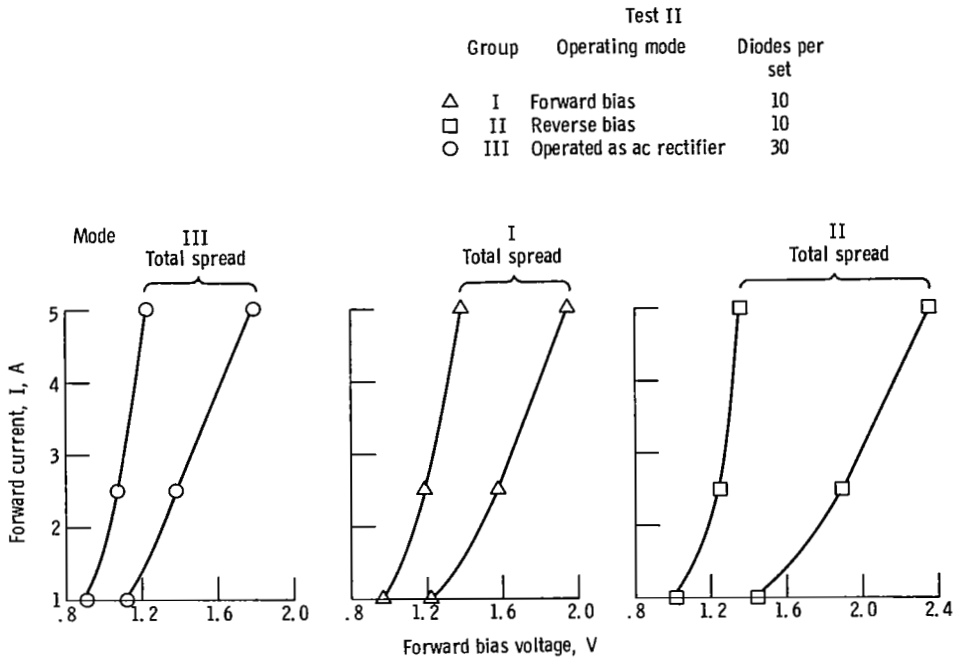

Figure 9. - Spread in forward voltage drops as function of different operating modes after diodes were irradiated.

(3) There is considerable spread in the forward voltage drops for currents in the ampere range after irradiation (see figs. 7 and 8).

(4) The amount of forward voltage drop for a given current is dependent on the mode of operation during irradiation. The average values of forward voltage drops for different operating modes are shown in figures 4 and 5, but the spread in values within each mode can be seen in figure 9 for test II. (Test I showed a similar change.) The envelope of the forward voltage drops within an operating mode has considerable spread and overlaps other operating mode envelopes. Each envelope then contributes considerably to the total spread shown in figures 7 and 8.

(5) The reverse-biased diodes (mode B) showed the greatest change in forward voltage drop at high injection levels and also the largest increase in current at bias levels below approximately 0.6 volt (see figs. 4 and 5).

Test II diodes showed a larger forward voltage drop for a given current at high current levels than that of test I diodes (see figs 4 and 5). The effect of temperature is inconclusive, however, since test II also had a neutron fluence approximately 6 percent higher than that of test I.

Theoretical analysis indicates that for diodes of this type (i.e., n^+-p-p^+ at high current levels) a voltage drop V_p occurs in the p-base, which is highly dependent on a geometric ratio formed by the base half-width d and the high-level diffusion length

L_{na} (ref. 8). Equation (B6) in appendix B shows this dependency. It can be shown by use of this equation that, if L_{na} decreases because of radiation so that d/L_{na} increases by a factor of 2.4, the voltage drop in the base increases from 0.116 to 1.27 volt. Combining this voltage drop with the calculated junction voltage after irradiation gives a total voltage drop of 1.87 volts. With reference to figures 4 and 5, this would be in reasonable agreement with the experimental results at 5 amperes. A somewhat smaller change is indicated for d/L_{na} in the modes A and C. Variation in d/L_{na} also offers a possible explanation of the considerable spread in the observed values of forward voltage drop with irradiation. Equation (B4) in appendix B is an expression for the forward current in a region of high injection:

$$I = \frac{2A_j q n_i D_{na}}{L_{na}} \tanh\left(\frac{d}{L_{na}}\right)\left[e^{q(V_A - V_P)/2kT} - 1\right]$$

The effect on the current of varying d/L_{na} can be seen by suitably normalizing I and plotting it as a function of d/L_{na} (fig. 10). The case considered herein is where $2A_j q n_i D_{na}/d$ = constant G and 1 is neglected in the bias region (>0.5 V).

Figure 10 shows a hypothetical case at a given forward bias for two diodes with the same forward current but different d/L_{na} ratios, as shown by the square and circular symbols on the curve. As the diodes are irradiated, the diffusion length decreases so that the ratios change considerably. After irradiation, the two values of forward current for the two diodes are shown by the solid square and circular symbols indicating a considerable difference in I for the same V_A. Or, stated another way, the necessary applied voltage for a given current would vary considerably. Although the values for both d and L_{na} are critical in determining the relation between the current and the voltage, d was assumed constant for the purposes of this analysis.

The foregoing discussion illustrates the possibility of increasing the radiation tolerance of these diodes both as to the uniformity of the forward electrical characteristics and to the magnitude of the change. By keeping $d/L_{na} < 0.9$ initially, the forward voltage drop for a given current should actually decrease with radiation. As L_{na} decreases to a value such that d/L_{na} is approximately 1 (fig. 10), the forward voltage drop will start to increase. To improve the uniformity of the forward electrical characteristics after irradiation, it is therefore necessary to closely control the d/L_{na} ratio. Controlling the base width d would be mainly a fabrication problem, whereas controlling the diffusion length L_{na} would involve both materials and fabrication processes.

Referring again to figures 4 and 5, it can be seen that after irradiation the plots of forward current as a function of applied voltage are no longer straight lines (i.e., ex-

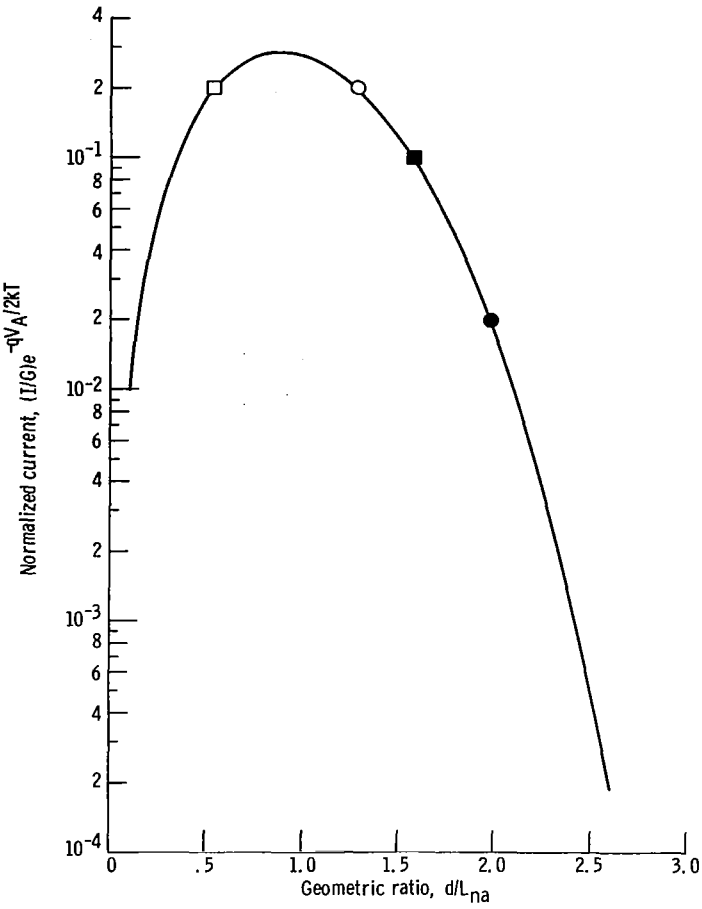

Figure 10. - Variation in forward current as function of geometric ratio at constant applied voltage.

ponential dependence of current on the applied voltage does not exist above 1 A). Shield's theory, as indicated previously, could account for the magnitude of the change in forward voltage drop at 5 amperes and the associated spread in values. It does not, however, predict the postirradiated slope. This suggests that there may be effects other than a change in base width, minority carrier lifetimes, and therefore, diffusion lengths that also affect the forward electrical characteristics of the diode. Neutron irradiation is known to introduce defects, lattice vacancies, and interstitial atoms that can act as traps to the majority carriers in the bulk semiconductor. In this case, the bulk region of interest is the base region. This process is known as carrier removal and has a twofold effect on the diode electrical characteristics. The first effect is to decrease the conductivity of the base region and therefore increase the forward IR drop across the base. This effect was considered and found to be negligible. The second effect is known as space-charge limiting (refs. 8 and 9), and it occurs when there is not an adequate

supply of majority carriers available for recombination at the edge of the n^+-p junction. The result is that, as a larger supply of electrons is injected into the base region, a local space charge is set up that tends to limit further injection and therefore to limit the current through the device. If this were the case, the following relation should apply:

$$I \propto K(V_A - V_B)^n$$

where K is a constant. The exponent n is 2 for a single-carrier and 3 for a double-carrier conduction (ref. 10). A curve showing the current as a function of voltage on a log-log plot is presented in figure 11. The value of 0.35 volt for the built-in voltage was determined experimentally from junction capacitance measurements as a function of applied voltages. The approximate straight lines and the slopes of approximately 3 indicate that space-charge limiting may be occurring. The slope values are reasonable when it is considered that the postirradiated curves are a composite of the effects of a changing d/L_{na}, the conductivity of the base, and space-charge limiting. The effects of space-charge limiting can be minimized at the current levels involved by again opti-

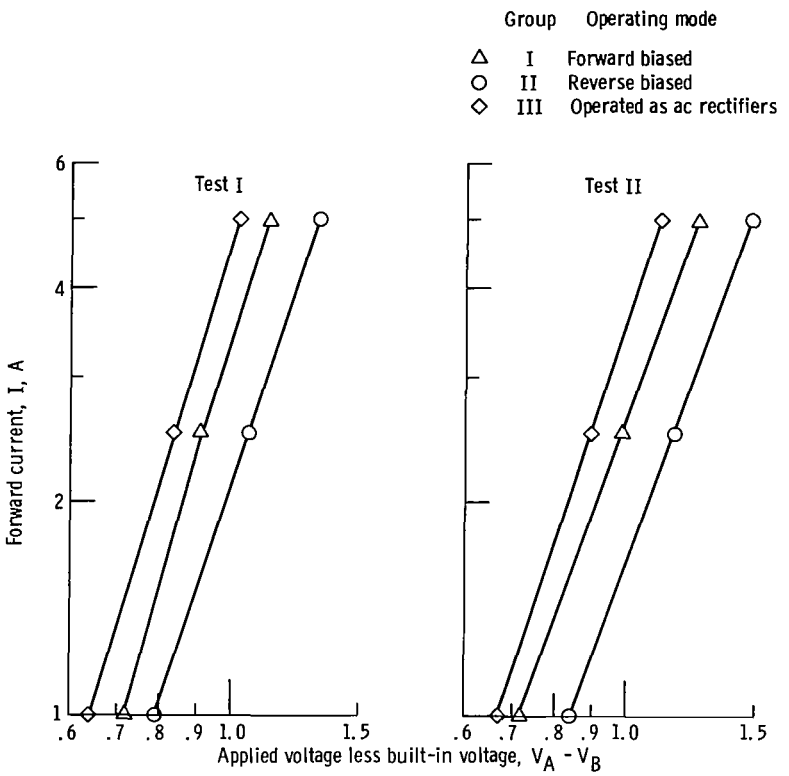

Figure 11. - Current-voltage relation for forward applied voltage minus built-in voltage after irradiation. Data points are average values by operating modes.

mizing d, since d is contained in the factor K. Increasing the doping level of the p-base region would also decrease the effects of space-charge limiting; however, a low enough level would have to be maintained to support reverse voltage breakdown.

SUMMARY OF RESULTS

The forward current-voltage characteristics of silicon power diodes irradiated at the NASA Plum Brook Reactor were analyzed in terms of existing theory. The following results were obtained:

1. The current-voltage characteristics agreed reasonably well with p-n junction theory based on generation-recombination and diffusion theories for low and medium levels of bias voltages.

2. After irradiation, the high-level currents were proportional to approximately the cube of the difference between the applied voltage and the built-in junction voltage. This relation suggests some form of space-charge limiting of the current.

3. The forward voltages at high-level currents before irradiation showed a very small variation among all the diodes tested, and the magnitudes of these voltages agreed reasonably well with theoretical calculations based on an n^+-p-p^+-type junction. After irradiation, however, there was considerable spread in the magnitudes of forward voltages for given currents, which probably resulted from the variation in the geometric radio d/L_{na} with radiation.

4. It appears that the radiation tolerance of the n^+-p-p^+-type silicon power rectifier can be improved by

   a. Controlling the minority carrier lifetime and, therefore, the diffusion length in the base region to attain consistency in the values of the low-level diffusion length for electrons in the p-region L_n

   b. Controlling the base widths as closely as possible for uniformity during fabrication

   c. Keeping the geometric ratio d/L_{na} as low as practicable during fabrication which, in turn, would require narrow base widths

   d. Increasing the base doping levels N_A to minimize space-charge limiting in the high-ampere current range

Lewis Research Center,
National Aeronautics and Space Administration,
Cleveland, Ohio, January 12, 1970,
120-27.

APPENDIX A

SYMBOLS

A_j	area of junction, cm^2
D_n	diffusion constant for electrons in silicon, cm^2/sec
D_{na}	high-level diffusion constant for electrons in silicon, cm^2/sec
d	one-half of base region width, cm
I	forward current, A
I_{ave}	average current, A
I_D	diffusion current, A
I_{rg}	generation-recombination current, A
k	Boltzmann's constant, eV/K
L_n	low-level diffusion length for electrons in p-region, cm
L_{na}	high-level diffusion length for electrons in p-region, cm
N_A	acceptor dopant concentration in p-region, cm^{-3}
n_i	intrinsic carrier concentration, cm^{-3}
n_p	density of electrons in p-region under thermal equilibrium conditions, cm^{-3}
q	charge on electron, K
T	temperature
V_A	applied voltage, V
V_B	built-in voltage at junction (diffusion potential), V
V_P	voltage drop in p-base region of diode, V
V_T	transition voltage, V
W	depletion region width, cm
τ	effective minority carrier lifetime, sec
τ_{no}	limiting lifetime for electrons in heavily doped p-region, sec
τ_{po}	limiting lifetime for holes in heavily doped n-region, sec

APPENDIX B

CALCULATION OF DIODE CURRENTS

Low-Level Forward Electrical Characteristics

Applied voltages below 0. 5 volt are not often of much interest so far as circuit applications are concerned, but current-voltage data in this region often furnish useful information as to the correctness of the theoretical approach and the physical parameters used.

The low-level current is essentially made up of three current components, generation-recombination, diffusion, and surface. In the bias region of zero bias up to approximately 25 millivolts, the surface component probably controls the current-voltage characteristics since the current at these biases is larger than would be expected from generation-recombination or diffusion theories. Above this bias up to approximately 0. 20 volt, both generation-recombination and diffusion components make comparable contributions so that, when the two calculated components are added, reasonable agreement is found with experimental values (fig. 3). From 0. 20 to approximately 0. 50 volt, the low-level diffusion component dominates with a transition region occurring between 0. 40 and 0. 50 volt, where the low-level diffusion goes to high-level diffusion.

The generation-recombination component of the forward current is due to the net generation-recombination of carriers in the depletion region of the n^+-p and p-p^+ junc-

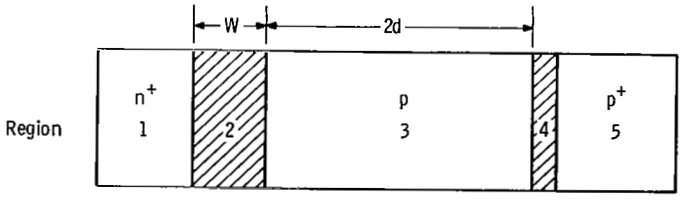

Figure 12. - Different dopant and depletion regions of n^+-p-p^+ silicon chip.

tions (regions 2 and 4, respectively, of fig. 12). The current contributed by the p-p^+ depletion region is small compared with that of the n^+-p so that only that component due to region 2 need be considered.

Sah et al. (ref. 11), in arriving at an expression for the generation-recombination current I_{rg}, integrated an expression for the net generation-recombination rate over the depletion region width. The resultant equation is

$$I_{rg} = \frac{2qn_i WA_j \sinh \frac{qV_A}{2kT}}{\sqrt{\tau_{po}\tau_{no}}\,(V_B - V_A)\,\frac{q}{kT}}\, f(b) \qquad \text{(B1)}$$

Evaluation of I_{rg} was made using the following values for the physical parameters:

Parameter	Value	Source
Area of junction, A_j, cm^2	0.455	Obtained from manufacturer
Intrinsic carrier concentration, n_i, carriers/cm^3	1.5×10^{10}	Reference 12
Depletion region width,[a] W, cm	4.5×10^{-4}	Value for zero bias obtained from junction capacitance measurements
$\sqrt{\tau_{po}\tau_{no}}$, sec	[b] 5×10^{-6}	Obtained from manufacturer
Built-in voltage at junction V_B, volts	0.35	Obtained from junction capacitance-voltage bias measurements
kT/q, volts, at 300 K	0.026	Calculated
f(b)[c]	0.05	Reference 11

[a] At zero and very low applied forward bias; decreases proportional to $V_A^{1/3}$ (ref. 10).

[b] An effective minority carrier lifetime.

[c] For very low applied bias; varies with voltage as

$$f(b) = \frac{1}{2\sqrt{b^2 - 1}} \ln \frac{b + \sqrt{b^2 - 1}}{b - \sqrt{b^2 - 1}} \quad \text{for} \quad b > 1$$

and

$$b = e^{\left(-qV_A/2kT\right)}108.5$$

where 108.5 was determined experimentally.

In this same bias region from 0.025 up to approximately 0.50 volt, the calculated diffusion current, which is summed with the generation-recombination component ($0.025 < V_A < 0.20$), is obtained from the low-level diffusion current expression (refs. 10 to 12):

$$I_D = \left(\frac{qAD_n n_p}{L_n}\right)\left(e^{qV_A/kT} - 1\right) \tag{B2}$$

From 0.20 volt up to the transition region, this component dominates (fig. 3). The transition from low to high level is indicated by the dashed lines. Equation (B2) applies to the type diode considered herein, where the n^+-region is much more heavily doped than the p-base. The following values for the various parameters were used in the calculations:

Parameter	Value	Source
Temperature, T, K	300	----------
Density of electrons in p-region under thermal equilibrium conditions, n_p, electrons/cm^3	1.6×10^6	Calculated from base doping, $n_p = \frac{(n_i)^2}{N_A}$
Diffusion constant for electrons in in silicon, D_n, cm^2/sec	30	Reference 12
Low-level diffusion length for electrons in p-region, L_n, cm	1.22×10^{-2}	Calculated from minority carrier lifetime, $L_n = \sqrt{D_n \tau_n}$

High Injection Level

In the high injection region of a p-n junction where the injected minority carriers (in this case, electrons at ~0.50 V) become comparable in number to the majority carrier density, a drift field is created that starts to alter the current-voltage relation (ref. 12). The diffusion equation (B2) becomes (ref. 12)

$$I_D = \frac{qA_j 2D_n n_i}{L_n} e^{qV/mkT} \tag{B3}$$

where $m = 2$ and the other constants have their values as given in the previous section. Equation (B3) is valid as long as the voltage drop in the lightly doped p-base is negligible. For the type of diode (n^+-p-p^+) considered herein, however, the drop in the base must be considered when calculating the current.

The experssion developed by Shields (ref. 8) for the forward current in a region of high injection for abrupt junctions takes into account this base voltage drop V_P:

$$I = \frac{2A_j q n_i D_{na}}{L_{na}} \tanh \frac{d}{L_{na}} \left(e^{q(V_A - V_P)/2kT} - 1 \right) \tag{B4}$$

This expression is a shortened form (ref. 8) of a more general equation, but it is applicable here under the conditions that d/L_{na} is approximately 1 and L_{na} and D_{na} are the high-current-level diffusion length and diffusion constant, respectively. Under these conditions, the current components due to recombination in the n^+- and p^+-regions are negligible. Equation (B4) holds above a transition voltage V_T given by

$$V_T = \frac{2kT}{q} \ln \frac{N_A}{n_i} \tag{B5}$$

where n_i is 1.5×10^{10} carriers per cubic centimeter (ref. 12), N_A is 1.4×10^{14} holes per cubic centimeter (furnished by manufacturer), and $2kT/q$ is 0.052 volt at 300 K. The value calculated for the transition voltage V_T was 0.48 volt. The expression for the voltage drop V_P in the base region can be expressed in terms of the geometry of the base (ref. 8):

$$V_P = \left(\frac{2kT}{q} \sinh \frac{d}{L_{na}} \right) \left(2 \arctan e^{d/L_{na}} - \frac{\pi}{2} \right) \tag{B6}$$

This equation can be used to evaluate L_{na} if it is assumed that the difference between the measured voltage drop across the diode at a given current and the calculated voltage using equation (B3) is the voltage drop V_P in the base. Using this calculated value of L_{na} and equation (B4), a comparison may be made between the measured and calculated values of the current and voltages. The following values were used to calculate L_{na}:

$$V_P = 0.116 \text{ V}$$

$$d = 9.4\times10^{-3} \text{ cm (from manufacturer)}$$

$$\frac{kT}{q} = 0.026 \text{ V at } 300 \text{ K}$$

The calculated value for L_{na} was 6.5×10^{-3} centimeter, and that for the ratio d/L_{na} was 1.45.

After the constant terms are evaluated, equation (B4) simplifies to

$$\tanh \frac{d}{L_{na}} = 0.89$$

and

$$\frac{2A_j q D_{na} n_i}{L_{na}} (0.89) = 4.9\times10^{-6}$$

$$I = 4.9\times10^{-6}\left[e^{q(V_A - V_P)/2kT}\right]$$

where the high-level value for D_{na} was taken as 16.3 square centimeters per second.

The values of voltages for given currents were calculated from equation (B4), and the foregoing constants were used to obtain the results given in table IV. Calculated currents over the range of 0.752 to 0.835 volt are given in table IV and are compared with average values.

TABLE IV. - CALCULATED VOLTAGES FOR HIGH-LEVEL CURRENTS

Current, I, A	Calculated voltage, V		Experimental average voltage, V
	Applied voltage less base voltage drop, $V_A - V_P$	Applied voltage, V_A	
5.0	0.719	0.835	0.82
2.5	.683	.799	.79
1.0	.636	.752	.75

REFERENCES

1. Messenger, George C.; et al: Device Performance Characteristics as Related to Radiation Damage in Semiconductor Materials. Rep. ARD-66-42-R, Northrop Corp. (AFCRL-66-462, DDC No. AD-643703), June 1966.
2. Larin, Frank: Radiation Effects in Semiconductor Devices. John Wiley & Sons, Inc., 1968.
3. Been, Julian F.: Effects of Nuclear Radiation on a High-Reliability Silicon Power Diode I - Change in I-V Design Characteristics. NASA TN D-4620, 1968.
4. Anon.: Screening Specifications for Semiconductor Device S1N1189. NASA Marshall Space Flight Center. Apr. 1963.
5. Davies, R. L.; and Gentry, F. E.: Control of Electric Field at the Surface of p-n Junctions. IEEE Trans. on Electron Devices, vol. ED-11, no. 7, July 1964, pp. 313-323.
6. Bozek, John M.; and Godlewski, Michael P.: Experimental Determination of Neutron Fluxes in Plum Brook Reactor HB-6 Facility with Use of Sulfur Pellets and Gold Foils. NASA TM X-1497, 1968.
7. Bozek, John M.: Experimental Determination of Gamma Exposure Rate in Plum Brook HB-6 Facility. NASA TM X-1490, 1968.
8. Shields, J.: The Forward Characteristics of p^+-n-n^+ Diodes in Theory and Experiment. Proc. IEE, vol. 106, pt. B, Suppl. 15, May 1959, pp. 342-352.
9. Jonscher, A. K.: Measurement of Voltage-Current Characteristics of Junction Diodes at High Forward Bias. J. Electr. Control, vol. 5, no. 3, Sept. 1958, pp. 226-244.
10. Lindmayer, Joseph; and Wrigley, Charles Y.: Fundamentals of Semiconductor Devices. D. Van Nostrand Co., Inc., 1965.
11. Sah, Chih-Tang; Noyce, Robert N.; and Shockley, William: Carrier Generation and Recombination in P-N Junctions and P-N Junction Characteristics. Proc. IRE, vol. 45, no. 9, Sept. 1957, pp. 1228-1243.
12. Phillips, Alvin B.: Transistor Engineering and Introduction to Integrated Semiconductor Circuits. McGraw-Hill Book Co., Inc., 1962.

NASA-Langley, 1970 — 26 E-5296